British Journal of Cancer www.nature.com/bjc

ARTICLE

Check for updates

Translational Therapeutics

Apalutamide radio-sensitisation of prostate cancer

Christos Kakouratos[1,3], Dimitra Kalamida[1,3], Ioannis Lamprou[1], Erasmia Xanthopoulou[1], Christos Nanos[1], Alexandra Giatromanolaki[2] and Michael I. Koukourakis[1]✉

INTRODUCTION: The combination of radiotherapy with bicalutamide is the standard treatment of prostate cancer patients with high-risk or locally advanced disease. Whether new-generation anti-androgens, like apalutamide, can improve the radio-curability of these patients is an emerging challenge.

MATERIALS AND METHODS: We comparatively examined the radio-sensitising activity of apalutamide and bicalutamide in hormone-sensitive (22Rv1) and hormone-resistant (PC3, DU145) prostate cancer cell lines. Experiments with xenografts were performed for the 22Rv1 cell line.

RESULTS: Radiation dose–response viability and clonogenic assays showed that apalutamide had a stronger radio-sensitising activity for all three cell lines. Confocal imaging for γH2Ax showed similar DNA double-strand break repair kinetics for apalutamide and bicalutamide. No difference was noted in the apoptotic pathway. A striking cell death pattern involving nuclear karyorrhexis and cell pyknosis in the G1/S phase was exclusively noted when radiation was combined with apalutamide. In vivo experiments in SCID and R2G2 mice showed significantly higher efficacy of radiotherapy (2 and 4 Gy) when combined with apalutamide, resulting in extensive xenograft necrosis.

CONCLUSIONS: In vitro and in vivo experiments support the superiority of apalutamide over bicalutamide in combination with radiotherapy in prostate cancer. Clinical studies are encouraged to show whether replacement of bicalutamide with apalutamide may improve the curability rates.

British Journal of Cancer (2021) 125:1377–1387; https://doi.org/10.1038/s41416-021-01528-1

INTRODUCTION

Prostate cancer is the most common tumour in men, reaching a pick incidence of 700–800 new cases per year, per 100,000 men aged >65 years [1]. The mortality, however, is fivefold lower as radical prostatectomy and radiotherapy provide high curability rates in the early stages of the disease [2]. Radiotherapy provides equivalent results to prostatectomy and is a widely applied treatment for patients with high-risk localised (T2, Gleason 8–10) cancer. Locally advanced (T3, T4, node-positive) stages of the disease are preferably treated with radical radiotherapy combined with androgen deprivation luteinising hormone-releasing hormone analogues and bicalutamide. Randomised trials have shown substantial prolongation of the overall survival time and improvement of the quality of life [3–6].

This synergistic effect of radiotherapy with ADT implicates that there is also a direct link between radio-resistance and androgen receptor (AR) pathway in prostate cancer. As Polkinghorn et al. demonstrated, AR signalling upregulates genes responsible for DNA repair, boosting prostate cancer cell's resistance to radiation [7]. Radiotherapy also appears to activate the AR. Spratt et al. showed that AR expression, nuclear localisation, and transcriptional activity increased after radiotherapy in vitro and in vivo. The induction of AR offered resistance to radiation and was associated with lower levels of DNA damage [8]. In addition, Goodwin et al. demonstrated that there is a positive loop between AR activity and DNA-dependent protein kinase, catalytic subunit, therefore DNA damage promotes faster DNA repair through AR [9]. These observations make clear the importance of combining radiotherapy with anti-androgens in clinical practice. Whether replacement of bicalutamide with more potent anti-androgens, such as enzalutamide [10] or apalutamide (ARN-509) [11], can improve the efficacy of radiotherapy on histologically aggressive and locally advanced prostate carcinomas is a question that is recently emerging.

Apalutamide binds selectively to ARs, with a 7–10-fold higher affinity than bicalutamide [12], preventing their nuclear translocation and activation of genes promoting tumour progression. Previous studies have shown that bicalutamide may exhibit androgen agonist effect in hormone-dependent prostate cancer cells [13]. Apalutamide, unlike bicalutamide, does not exhibit antagonist-to-agonist switch [12]. In 2018, Food and Drug Administration approved apalutamide for the treatment of asymptomatic non-metastatic castration-resistant prostate cancer, following the 'SPARTAN' trial that showed improved metastasis-free survival and longer time to develop symptoms [14]. More recently, its approval was extended for the treatment of patients

[1]Department of Radiotherapy/Oncology, Democritus University of Thrace, Alexandroupolis, Greece. [2]Department of Pathology, Democritus University of Thrace, Alexandroupolis, Greece. [3]These authors contributed equally: Christos Kakouratos, Dimitra Kalamida. ✉email: targ@her.forthnet.gr

Received: 24 February 2021 Revised: 30 July 2021 Accepted: 11 August 2021
Published online: 1 September 2021

with metastatic castration-sensitive prostate cancer, following the randomised 'TITAN' trial that confirmed significant improvement in the radiographic progression-free survival over androgen deprivation therapy [15].

This study aims to investigate comparatively the effects of bicalutamide and apalutamide on the radiation sensitivity of prostate cancer cells. The androgen-dependent 22Rv1 cell line was studied in parallel with the DU145 and PC3 androgen-independent cell lines [16].

MATERIALS AND METHODS

Cell lines

Three prostate cell lines are selected according to their response to testosterone, as previously described [16] (the androgen-independent DU145 and PC3 and the androgen-dependent 22Rv1 cell lines). The 22Rv1 cell line was purchased from ATCC (https://www.lgcstandards-atcc.org/Products/All/CRL-2505.aspx). The PC3 and DU145 cell lines were purchased from the CLS Germany (http://clsgmbh.de/p1699_PC-3.html and http://clsgmbh.de/p708_DU-145.html). Additionally, a certificate of authentication of cell lines was granted by the Eurofins-Forensik, Germany.

Exposure to testosterone and anti-androgens

Testosterone (Alpha-Pharma Healthcare, Chandivali, Mumbai, 400072, India) was used at 10 nM. Bicalutamide (RAFARM, Athens, Greece) and apalutamide/ARN-509 (Janssen Pharmaceutica NV) were dissolved in dimethyl sulfoxide (DMSO) at a concentration of 50 mM and used at 10 μM for the in vitro experiments. A similar concentration was also applied for bicalutamide (10 μM). Higher concentrations of 25 μM and 50 μM were also applied for apalutamide to investigate an eventual dose-dependent radio-sensitising effect.

The concentration of 10 μM apalutamide was selected according to our previous study, in which this concentration had a minor effect on cell proliferation [16]. Concentrations of this range have been used in several other studies with second-generation anti-androgens. Elsesy et al. used apalutamide at concentration range of 20–40 μM, while Sekhar et al., Triggiani et al., and Ghashghaei et al. used enzalutamide at a concentration of 10 μM [17–20]. Despite the in vitro data showing a higher binding affinity of apalutamide over bicalutamide [12], the dose of apalutamide established for the treatment of prostate cancer patients is 240 mg/day [14, 15], which is higher than the clinically used 50–150 mg/day of bicalutamide.

Post-irradiation proliferation-viability experiments

For proliferation experiments, cell viability was measured using AlamarBlue® assay, a method that has been previously validated by our group [21]. AlamarBlue® assay is an easy, reliable non-toxic, and safe method to measure cell viability. The method relies on the metabolic activity of the cells to reduce resazurin (weakly fluorescent) to resorufin (highly red fluorescent). The reduction is performed by mitochondrial enzymes. Briefly, 10% v/v AlamarBlue is added to each well, and after a 7-h incubation, fluorescence is measured (excitation: 530–560 nm and emission: 590 nm) with the FLUOstar Omega filter-based multi-mode microplate reader (BMG Labtech). For each dose, six wells with irradiated cells are monitored, and the mean value was used to plot the dose–response curves.

The viability of prostate cancer cells was initially characterised following exposure to multi-dose irradiation (2–15 Gy). This range of doses starts from the dose of 2 Gy applied clinically in standard fractionation radiotherapy schemes and increases to 4–6 Gy used in hypofractionated schemes and went up to 16 Gy, to achieve around 100% lethality for the tested cell lines. Cells were seeded in a 96-well plate at a density of 250 cells per well. Following the protocol of multi-dose irradiation of the well columns within the same 96-well plate [22], exposure of cells to radiation was performed using a 6 MV beam of a Linear Accelerator (PRECISE, ELEKTA) endowed with a MultiLeaf collimator.

Cells were incubated for 3 h to allow attachment on the surface of the wells. Cells were then incubated with anti-androgens (at 10 μM) for 4 days (1 day before the RT and 3 days after the RT) in culture medium with or without testosterone (10 nM). For apalutamide, higher concentrations (25μM and 50 μM) were also tested to assess the eventual dose-dependence effect on radio-sensitisation. After the first 24 h, cells were irradiated with 3, 6, 9, 12, and 15 Gy, and the viability of cells on day 7 (the day of the nadir of cell counts) was used to create radiation dose–response curves.

Although PC3 and DU145 cell lines are considered hormone independent, we decided to also investigate the addition of testosterone in the in vitro experiments. We believe it is important to simulate the human body environment where testosterone levels are substantial. By simulating this condition in in vitro experiments, we could obtain more reliable results regarding the radio-sensitivity of these cell lines.

Clonogenic assays

Cells were trypsinised and seeded into 24-well plates at appropriate density (25 cells per well) in triplicates. Cells were then incubated for 3 h to allow attachment on the surface of the wells and then were treated with apalutamide for 4 days (1 day before the RT and 3 days after the RT) (at 10 μM). Following 24 h treatment, cells were irradiated using 0, 3, 6, 9, and 15 Gy. Plates were then placed in the incubator, and the medium was changed every 3 days. Irradiation of plates was performed using a 6 MV X-ray beam of a Linear Accelerator (Precise; Elekta, Stockholm, Sweden). Fourteen days after irradiation, the medium was removed, and cells were washed with 2 ml of phosphate-buffered saline (PBS). Subsequently, the cells were fixed by adding 2 ml of 100% methanol for 10 min at −20 °C and stained with 0.5% w/v Crystal Violet (Sigma-Aldrich, Taufkirchen, Germany) in 25% methanol for 10 min. The cells were then washed several times with distilled water, and colonies with at least 50 cells were counted on an inverted microscope. The plating efficiency, the percentage of seeded cells producing colonies, was then calculated.

Apoptosis imaging

Apoptosis has been detected by Annexin V (green fluorescence Ex/Em = 490/525 nm), a phosphatidylserine indicator on the cell surface, using the Apoptosis/Necrosis Detection Kit (blue, green, red) (ab176749) (Abcam, UK) and Cell-IQ MLF live imaging system. The kit has been used according to the manufacturer's instructions. Untreated cells have been used as a control and treated cells for 24 h with 1 μM Docetaxel, an anti-cancer chemotherapy taxane drug, was used as a positive control for apoptosis induction. DU145, 22Rv1, and PC3 cancer cell lines have been irradiated with 4 Gy for DU145 and 22Rv1 and 10 Gy for PC3, and apoptosis has been monitored at several time points. The fluorescence images have been merged, and the fluorescence intensity has been quantified using ImageJ 1.47v (National Institute of Health, USA), and graph presentation has been performed using the GraphPad Prism Version 5.01a statistical package (GraphPad Software Inc., USA).

Confocal microscopy studies

For immunofluorescence staining and monitoring nuclear catastrophe and double-strand DNA damage, DU145, 22Rv1, and PC3 cancer cell lines were grown on No. 1.5 glass coverslips, treated with the appropriate drug, and irradiated using 4 Gy for DU145 and 22Rv1 and 10 Gy for PC3. PC-3 cell line exhibits high resistance to radiation in comparison to DU145 and 22Rv1 cell lines (see Fig. 1). For the assessment of γH2ax kinetics as well as for the nuclear catastrophe study, we chose to expose each cell line to a single radiation dose approximately equal to radiation dose producing 50% cell viability reduction (RD50).

The cells were then fixed after set time points in 3.7% paraformaldehyde/PBS pH 7.4 for 20 min at 37 °C and then permeabilised in PBS/0.1% v/v Triton X-100 pH 7.4 for 5 min at room temperature (RT). In addition, cells were blocked in PBS/5% w/v bovine serum albumin pH 7.4 for 20 min and stained with various primary antibodies: anti-gamma H2AX (phospho S139) antibody rabbit polyclonal (1:500; Abcam), anti- alpha-tubulin rabbit polyclonal (1:1000;Abcam), and anti-Ki67 mouse monoclonal (1:150; DAKO) for 1 h at RT. Cells were washed in PBS pH 7.4, incubated with appropriate CF 488 and 564 secondary antibodies at RT, and DNA was counterstained with Hoechst 33342 (1 μg/ml; Sigma-Aldrich). After final washes, coverslips were mounted in a homemade Mowiol mounting medium. Imaging was performed on a customised Andor Revolution Spinning Disk Confocal System built around a stand (IX81; Olympus) with a ×60 lens and a digital camera (Andor Ixon+885) (CIBIT Facility, MBG-DUTH). Image acquisition was performed using the Andor IQ 2 software. Optical sections were recorded every 0.3 μm. All confocal microscopic images presented in this work are two-dimensional (2D) maximum intensity projections of *z*-stack images, and image analysis for the obtained data sets has been performed using ImageJ 1.47v (National Institute of Health, USA). Image analysis and quantification of Ki67 and γH2Ax expression have been performed using

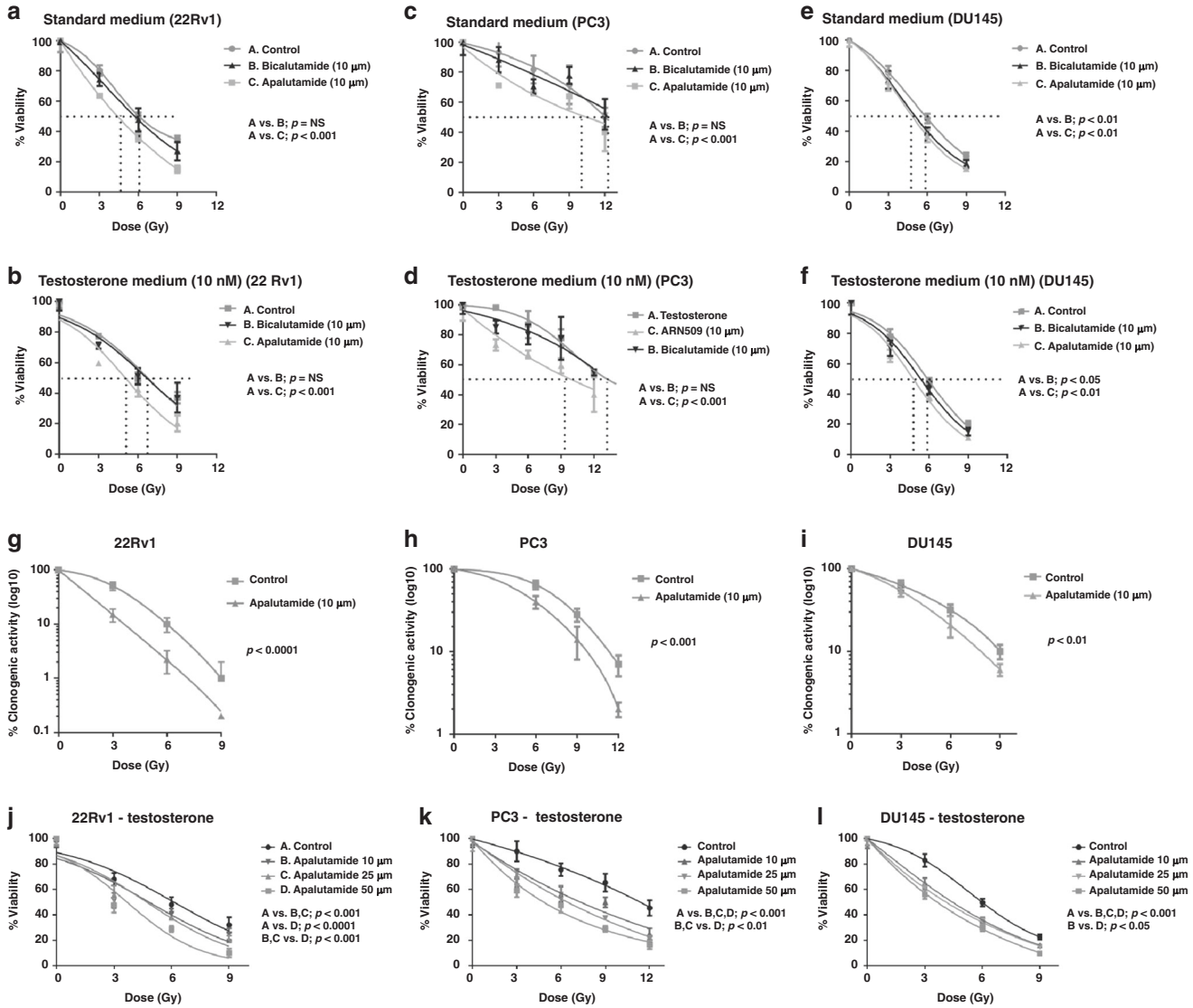

Fig. 1 Apalutamide radio-sensitises PCa cells in vitro. Viability radiation dose–response curves of the 22Rv1, PC3, and DU145 prostate cancer cell lines, exposed to bicalutamide, apalutamide, or no drug (control), in standard medium (**a**, **c**, **e**) and testosterone-enriched medium (**b**, **d**, **f**). Clonogenic radiation dose–response curves of 22Rv1, PC3, and DU145 prostate cancer cell lines exposed to apalutamide (**g**, **h**, **i**). Viability radiation dose–response curves of 22Rv1, PC3, and DU145 prostate cancer cell lines exposed to escalated doses of apalutamide in testosterone-enriched medium (**j**, **k**, **l**).

custom-developed macros in the ImageJ software 1.47v (National Institute of Health, USA). A population of n cells ($n \geq 30$) has been analysed. The 2D average projection of z-stack images was quantified while fold increase compared to the control was measured in both cases. Graph presentation has been performed using the GraphPad Prism Version 5.01a statistical package (GraphPad Software Inc., USA).

Assessment of DNA double-strand break kinetics

The 22Rv1, PC3, and DU145 prostate cancer cell lines were cultured for 24 h, with and without anti-androgens (at 10 μM), and then irradiated. Given the different radio-sensitivity noted for the three cell lines, a dose of 4 Gy was applied to DU145 and 22Rv1 and a dose of 10 Gy to the PC3 cell line. The formation and regression in time of γH2Ax nuclear foci was monitored at 30 min, 4 h, and 24 h after irradiation, using confocal microscopy. Custom-developed macros in the ImageJ software 1.47v (National Institute of Health, USA) were applied for quantification.

Western blot studies

Whole-cell lysates were prepared in lysis buffer with Triton X-100 (10 mM HEPES, 60 mM KCl, 1 mM EDTA, 0.1% (v/v) Triton X-100, pH 7.6) containing fresh protease inhibitors and phosphatase inhibitors. Proteins of each lysate were resolved by discontinuous sodium dodecyl sulfate gels and transferred to polyvinylidene difluoride membranes. Following blocking in 5% non-fat dried milk for 2 h at RT, membranes were incubated at 4 °C overnight with the appropriate primary antibodies. The membranes were then incubated for 2 h at RT with the secondary antibody. For the assessment of cell cycle arrest and apoptosis induction, we used an antibody cocktail (ab139417, Abcam, UK) containing four primary antibodies, targeting Cdk2 pTyr15 (G1/S arrest), Histone H3 pSer10 (M-phase arrest), cleaved poly ADP-ribose polymerase (PARP), and Actin. The secondary antibody was a mixture of horseradish peroxidase-conjugated antibodies (anti-mouse and anti-rabbit) and is also provided by the kit (ab139417). The images of the blots were captured utilising ChemiDoc™ MP imaging system (Bio-Rad, Hercules, CA); quantification was performed using the Image J software (ImageJ 1.49v; National Institute of Health, USA).

Development of 22Rv1 fluorescent cell line

The development of a stably transfected 22RV, PC3, and DU145 prostate cancer cell line was achieved using a second-generation Lentiviral system. In this procedure, we used a Lentivirus-based vector expressing the

mCherry protein, along with resistance genes for two antibiotics (Puromycin and Ampicillin). The plasmid was purchased from GenePharma (Shanghai GenePharma, China). The plasmid vector was amplified using the DH5-Alpha competent bacteria cells, followed by antibiotic selection of the successfully transformed clones using Ampicillin (Amp). Subsequently, the extraction of plasmid DNA was performed using the NucleoSpin Plasmid Miniprep Kit (REF# 740588.10, Macherey-Nagel, Germany).

Afterwards, the Lentivirus particles were produced by transient co-transfection of HEK293 host cells with the Lentiviral vector [LV10N(U6/mCherry&Puro&Amp)] together with the packaging plasmid (pCMVR8.74) and the envelope plasmid (pczVSV-G). The supernatant containing Lentiviruses was collected, centrifuged at $1000 \times g$ for 10 min, followed by filtration through a 0.22 µm filter and stored in aliquots at −80 °C or immediately used to infect target cells. After a single round of infection, the successfully infected cells were selected using Puromycin (4 µg/ml) and further passaged in culture. Moreover, western blot for AR (ab9474, Abcam, Cambridge, UK) was performed to confirm that the infected 22Rv1 cells still express functional, testosterone-sensitive AR (Supplemental Fig. S1).

Animal handling

Two genetically engineered and mutated mice (GEMM) strains, the NOD SCID (NOD.CB17-Prkdc$^{scid/}$J, Genotype: HOM Homozygous for Prkdc^{scid}) and R2G2 (B6.129-Rag2^{tm1Fwa} Il2$^{rg\ tm1Rsky}$/DwlHsd) were used for the in vivo experiments. These are immunodeficient mouse models that lack functional T cells and B cells. The R2G2 mouse model also lacks natural killer cells and has a deficiency in lymphocyte development. On the other hand, the NOD SCID model carries a DNA repair defect that makes it more sensitive to ionising radiation.

Animal care and handling were carried out according to the guidelines set by Directive 2010/63/EU. The study has been approved by the local Animal Experimentation Research Committee and the Ethics Committee of the Democritus University of Thrace. The Veterinary Direction also approved all experimental procedures for Animal Research in the Department of Experimental Surgery at the Democritus University of Thrace. Mice were housed in ventilated cages (Easy Flow IVC Air Handling Unit, Tecniplast) with standard rodent chow, water, and 12 h light–dark photoperiod under an ambient temperature of 23 °C.

For the euthanasia, the animals were anaesthetised using ketamine (70 mg/kg via intraperitoneal injection) followed by cervical dislocation.

For the experiments, male 8-week-old mice were used. As xenografts were implanted at the flank of mice, lower body (below thorax) irradiation was applied using a LINAC 6MV (ELEKTA). The irradiation method of the lower body that does not demand anaesthesia has been previously published by our group [23].

Before proceeding with xenograft experiments, the radio-tolerance of both strains was studied following a single fraction of 2, 4, or 6 Gy directed to the lower mouse body. Supplemental Fig. S2 shows the survival curves of mice plotted against the days of follow-up after irradiation. Following abdominal irradiation with 2 Gy, 1/7 Nod SCID mice died vs. 0/7 of R2G2 mice. At 4 Gy, only 1/7 Nod SCID mice survived, while all R2G2 mice were alive 20 days after irradiation. At 6 Gy, all Nod SCID mice died, while R2G2 mice exhibited remarkable survivability as all irradiated mice were alive at 20 days. The period of 20 days is the critical period beyond which no deaths are expected.

Based on the above data, we decided to perform the experiments with both NOD-SCID and R2G2 mice, delivering 2 and 4 Gy, respectively. This would allow the study of radio-sensitisation of apalutamide with daily radiation doses used in clinical standard fractionation regimens (2 Gy/day) and in hypofractionated radiotherapy (4 Gy/day).

Xenograft experiments

Xenograft experiments were performed with the 22Rv1 hormone-sensitive cell line only, which shows the best response to apalutamide. Hormone-sensitive disease represents the majority of newly diagnosed prostate carcinomas referred for radiotherapy. It was, therefore, suggested that focussing on the 22Rv1 cell line and expanding experiments with two different dose schedules in two distinct mouse strains (SCID and R2G2 mice) would be more relevant to the aims of the xenograft phase of the study and would better comply to the 3R conditions of experimentation with animals (replacement—reduction—refinement). The decision to include two different strains of animals, including the very radio-sensitive SCID strain, was made as this would allow the study of eventual abdominal normal tissue damage or even out-of-radiotherapy field normal tissue toxicity of apalutamide.

Four cohorts of seven R2G2 mice and of seven SCID mice each were established, and mice were injected with 5×10^6 cells at their flank. Animals were monitored every 3 days after implantation, and when the tumour size reached about 0.75 cm^2, animals were treated with placebo (solvent without drug) or anti-androgens (bicalutamide 50 mg/kg, apalutamide 50 mg/kg, and apalutamide 250 mg/kg). Apalutamide was dissolved in DMSO and then were further diluted with corn oil to a final ratio of 10% DMSO and 90% corn oil. Dilution in corn oil solution prevented skin reactions to apalutamide. Bicalutamide was dissolved in water-for-injections. Although in other in vivo studies second-generation anti-androgens were administered at lower concentrations over longer periods of time [19, 24], in this study we decided to simulate the daily dose delivered to humans (240 mg/day equivalent to 4 mg/kg for a 60 kg man) in the mouse condition. This is achieved by dividing the animal dose by 12.3 [25], so that the dose of 50 mg/kg in mice gives an equivalent of 4 mg/kg in man.

Placebo (DMSO in corn oil) or drugs were injected for 4 consecutive days (day −2, −1, 0, and 1). Lower body irradiation with 2 Gy and with 4 Gy was delivered on day 0 (without anaesthesia) for SCID and R2G2 mice, respectively. The growth of xenografts was recorded on days 0 (day of irradiation; immediately before irradiation), 3, 7, 10, and 14 with the IVIS kinetic imaging system (Real-Time Fluorescent & Bioluminescent Fast Imaging; Perkin Elmer-Caliper Life Sciences, USA), using fixed settings for every imaging session (Exposure time: 0.042 s, Binning Factor: 4, Excitation Filter: 560 nm, Emission Filter: 620 nm, *f* Number: 2, Field of View: 10, EM Gain: 50). The tumour area in each image was defined as the region of interest detected with a threshold of 10–30% radiant efficiency using the Living Image® 4.7.4 software (Caliper Life Sciences). The relative growth rate was calculated using the measurements (area in cm^2) of day 0 and scoring the obtained dimensions as 1. The ratio of 'day *x*'/'day 0' provided the tumour's relative growth on each day '*x*'.

Pathology studies

Four SCID and R2G2 mice from each above-described treatment groups were sacrificed on day 10. Tumours were excised, placed in formalin for fixation, and sent to our Pathology department for inclusion in blocks of paraffin and histological examination. Sections were cut at 3 µm and stained with haematoxylin and eosin. The percentage of tissue with necrosis was assessed in all ×10 optical fields, and the mean value of all fields was calculated to score each tumour. The number of optical fields per tumour ranged from 5 to 8 depending on size.

Statistical analysis

Statistical analysis and graph presentation were performed using GraphPad Prism 7.0 (GraphPad Software Inc., USA). The unpaired two-tailed *t* test or the Wilcoxon matched-pairs test were used to compare groups with continuous variable data, as appropriate. One-way analysis of variance non-parametric analysis (Kruskal–Wallis test) was also performed to test differences among groups of continuous variables. A p value of <0.05 was used for significance. All in vitro experiments were repeated three times.

RESULTS

Radiation dose–response curves in the presence of anti-androgens

The response of cancer cells to radiation was compared to cells incubated for 4 days with apalutamide or bicalutamide (10 µM for 1 day before irradiation and 3 days thereafter). Same experiments were performed with cells growing in testosterone-containing medium (10 nM). The presence of testosterone was allowed for all 4 days of incubation together with the drugs.

22Rv1 cells growing under standard culture medium showed a radiation dose-dependent reduction of viability (AlamarBlue® assay), while bicalutamide per se had no effect on the growth kinetics (Fig. 1a). On the contrary, cells incubated with apalutamide showed a significant reduction of post-irradiation viability ($p < 0.001$). The RD50 was reduced from 6.1 Gy down to 4.3 Gy.

22Rv1 cells growing under the presence of testosterone (10 nM) also showed radiation dose-dependent reduction of viability (Fig. 1b). Viability of cells was slightly increased compared to the one noted in cells growing in testosterone-free medium (RD50 6.8 vs. 6.1 Gy). Post-irradiation viability was not affected by the incubation with

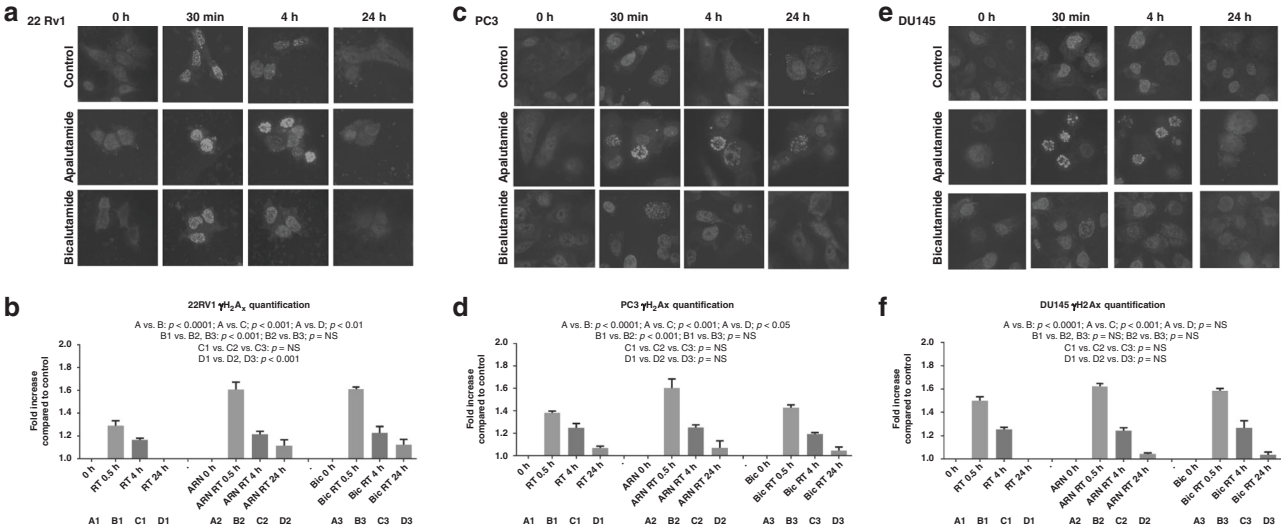

Fig. 2 γH2Ax kinetics in prostate cancer cells post radiation with or without anti-androgens. Fluorescent immunocytochemical images of 22Rv1 (**a**), PC3 (**c**), and DU145 (**e**) cell lines, stained for γH2Ax, at 0 h, 30 min, 4 h, and 24 h after exposure to radiation (4 Gy to the 22Rv1 and DU145 cell lines and 10 Gy to the PC3 cell line). The kinetics of the intensity of γH2Ax fluorescence in cell nuclei is plotted (**b**, **d**, **f**).

bicalutamide. On the contrary, cells incubated with apalutamide showed a significant reduction of viability ($p < 0.001$). The RD50 was reduced from 6.8 Gy down to 5.2 Gy ($p < 0.001$).

Similar results were obtained in experiments with the PC3 and DU145 cell lines (Fig. 1c–f). Bicalutamide produced a marginal non-significant effect on post-irradiation cell viability. For the PC3 cell line, apalutamide reduced the RD50 from 12.3 to 10.1 Gy and from 13.2 down to 9.7 Gy in the absence or in the presence of testosterone, respectively ($p < 0.001$). For the DU145 cell line, the effect was less intense; still, apalutamide reduced the RD50 from 5.83 to 4.60 Gy and from 5.87 to 4.83 Gy in the absence or in the presence of testosterone, respectively ($p < 0.001$). Bicalutamide also produced a significant reduction ($p < 0.01$).

Clonogenic assays were performed further to test the efficacy of apalutamide as a radio-sensitiser. Cell lines were subsequently irradiated with 3, 6, and 9 Gy, and the development of colonies was studied 14 days after irradiation. Apalutamide significantly reduced all irradiated cell lines' clonogenic capacity, the maximum effect shown for 22Rv1 cells ($p < 0.0001$); Fig. 1g–i.

Radiation dose–response viability curves under apalutamide dose escalation

To further investigate the eventual dose effect of apalutamide on the combined apalutamide/radiotherapy efficacy against the three prostate cancer cell lines, we further increased the dose of apalutamide to 25 and 50 μM and obtained relevant radiation dose–response curves (Fig. 1).

For the 22Rv1 cell line, the escalation of apalutamide dose to 50 μM produced a significant enhancement of the combination's efficacy (Fig. 1j). The same effect was evident for the PC3 cell line (Fig. 1k), while a smaller, still significant effect was noted in the DU145 one (Fig. 1l).

Assessment of DNA double-strand break kinetics

The formation and regression in time of γH2Ax nuclear foci were monitored at 30 min, 4 h, and 24 h after irradiation (4 Gy to the 22Rv1 and DU145 cell lines and 10 Gy to the PC3 cell line, as reported in 'Materials and methods'). All cell lines showed a significant increase of γH2Ax foci 30 min after irradiation (with and without the presence of anti-androgens). The intensity of the spots declined rapidly at 4 and 24 h (Fig. 2a–c).

In the 22Rv1 cancer cell line, there was a significant higher formation of γH2AX foci in the presence of all anti-androgens compared to radiation alone ($p < 0.0001$) (Fig. 2a). At 24 h, there was a remnant presence of γH2Ax foci, only when cells had been irradiated under the presence of anti-androgens ($p < 0.05$). No difference was noted between apalutamide and bicalutamide.

In the PC3 cancer cell line, there was a significant higher formation of γH2Ax foci in the presence of apalutamide compared to radiation alone and bicalutamide ($p < 0.001$). Bicalutamide did not alter the patterns of γH2Ax kinetics compared to radiation alone (Fig. 2b). At 24 h, there was a small remnant presence of γH2Ax foci, which was, however, similar whether the cells received radiation with or without anti-androgens.

In the DU145 cancer cell line, there was a higher formation of γH2Ax foci in the presence of apalutamide, but this did not reach significance (Fig. 2c). No difference was noted at 4 and 24 h between cells that received radiation with vs. without anti-androgens.

Karyorrhexis and pyknosis after irradiation with apalutamide

An unexpected finding was recorded in all three cell lines receiving radiation with apalutamide. At 30 min and 4 h after irradiation, there was a striking abundance of cells with clearly disorganised nuclei and strong localisation of γH2AX in large round 'pearl-like' structures that corresponded to fragmented parts of the nuclei (Fig. 3). This pattern is also evident in Fig. 2. Such cells persisted 24 h after irradiation, although the γH2Ax presence vanished. This observation suggested the induction of a specific death pattern, starting as early as 30 min after irradiation when this latter was combined with apalutamide. Neither the radiation alone nor radiation combined with bicalutamide provided a cell-damaging and death pattern of this type.

We further investigated the above recorded apalutamide-specific radiation-induced death pattern by performing double immunostaining for the Ki67 nuclear antigen (widely used as a proliferation nuclear marker) and tubulin (a protein expressed in the cytoskeleton of the cytoplasm, but not in the nuclei). Prostate cancer cells from the three cell lines were cultured for 24 h with or without the presence of apalutamide and then irradiated (4 Gy for the DU145 and 22Rv1 and 10 Gy for the PC3 cell line). Twenty-four hours later, cells were fixed, undergone double immunostaining for Ki67 and tubulin, and examined under confocal microscopy. An abundant presence of dying cancer cells, sharing the 'pearl-like' morphological and immunocytochemical characteristics, was

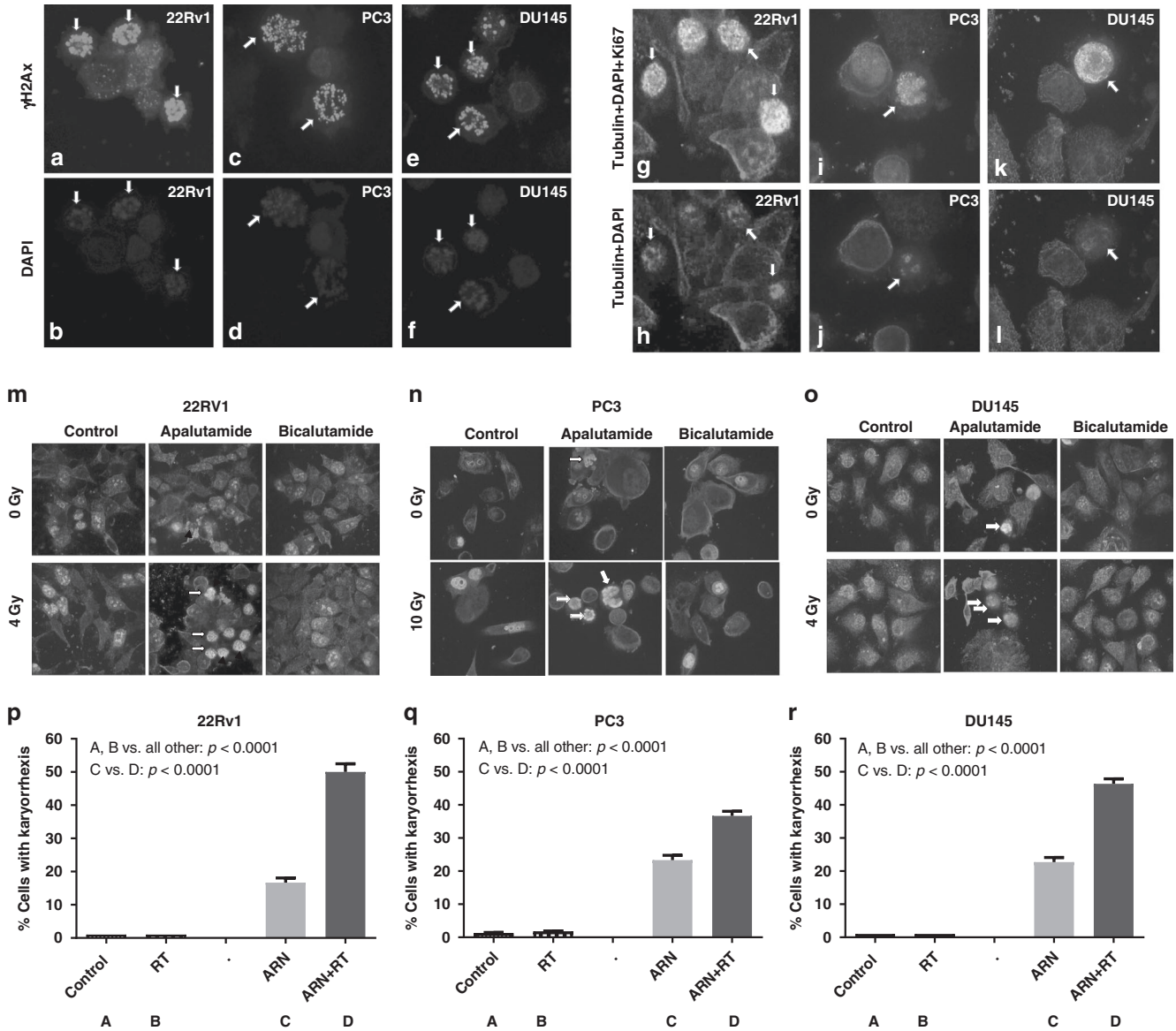

Fig. 3 γH2Ax abnormal localisation and nuclear catastrophe following apalutamide exposure and cell irradiation. Immunofluorescent confocal microscopy images and quantification analysis: **a**, **c**, **e** show γH2Ax red immunostaining for 22Rv1, PC3, and DU125 prostate cancer cells 24 h after exposure to apalutamide and radiation, respectively, while **b**, **d**, **f** show the same DAPI (blue nuclear staining) images. Arrows point to the pearl-like karyorrhexis of the nuclei. **g**, **i**, **k** show double immunostaining with anti-Ki67 and anti-tubulin (cytoplasm staining) antibodies (**h**, **j**, **l** show the same images with DAPI and tubulin only staining). Arrows point to pyknotic cells with karyorrhexis, where the fragmented nuclei (stained green with Ki67) are dislocated to the periphery of the cells, while the cytoplasm stained red with tubulin is intercalated among fragments. **m**, **n**, **o** show typical double immunostaining with tubulin/Ki-67 of 22Rv1, PC3 and DU145 cell lines, respectively, treated with apalutamide and bicalutamide, with or without irradiation. Arrows show the pyknotic cells with karyorrhexis that are evident in the apalutamide/irradiation-treated cells. **p**, **q**, **r** show the quantification of the percentage of cancer cells with karyorrhexis in 22Rv1, PC3, and DU145 cells, respectively, exposed to radiation, apalutamide (ARN), and their combination.

recorded (Fig. 3). These characteristics can be summarised as follows:

1. Pyknosis with shrinkage and condensation of the cell size by around 50% of initial dimensions;
2. Karyorrhexis with nuclear fragmentation;
3. Intense expression of the Ki67 protein in the nuclear fragments;
4. Dislocation of the nuclear fragments to the cell periphery;
5. Engulfment of cytoplasm expressing the tubulin in central cell areas or among the nuclear fragments.

Quantification of these cells exhibiting karyorrhexis (Fig. 3) showed that these were absent in untreated cells or cells treated with radiation alone or with bicalutamide in all three cell lines. Exposure of cells to apalutamide alone resulted in a significant increase of this cell subpopulation from 0 to 16 ± 4, 23 ± 5, and 23 ± 5% in the 22Rv1, PC3, and DU145 cells, respectively ($p < 0.0001$). The addition of radiotherapy to apalutamide-incubated cells resulted in a sharp, significant increase of the cell population with karyorrhexis, to 50 ± 8, 36 ± 5, and 45 ± 5% in the 22Rv1, PC3, and DU145 cells, respectively ($p < 0.0001$).

Apoptosis after irradiation with apalutamide

Cell lines were subsequently irradiated as above (4 Gy for 22Rv1 and DU147 and 10 Gy for PC3) and the rate of apoptotic cells was recorded at 2 h, 4 h, 24 h, and 4 days, thereafter. The Apoptosis

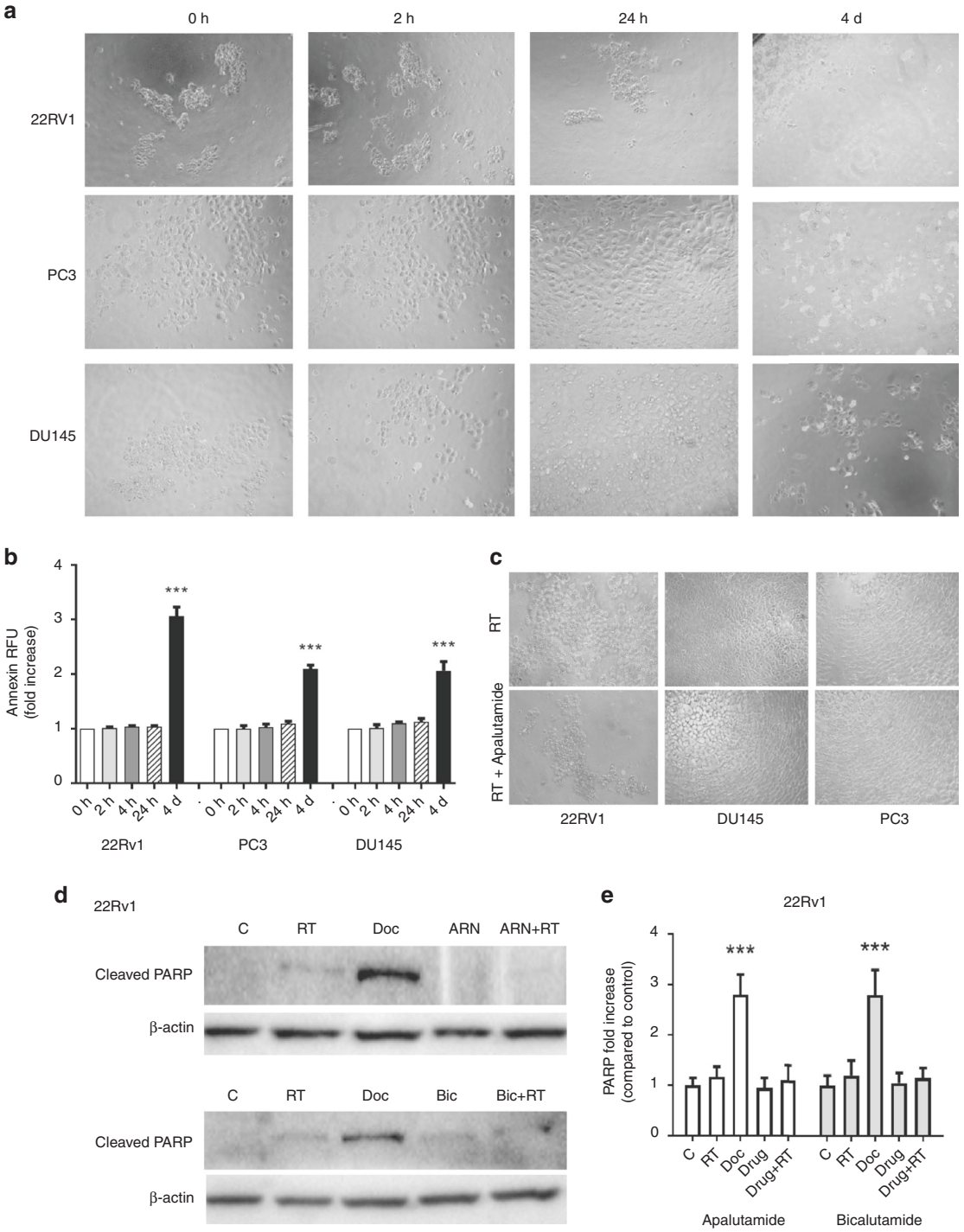

Fig. 4 Combination of apalutamide with radiation does not induce an early apoptotic response. Analysis of apoptosis markers of 22Rv1, PC3, and DU145 prostate cancer cell lines, exposed to radiation (4 Gy for 22Rv1 and DU147 and 10 Gy for PC3): **a** typical images of apoptotic cells stained with Annexin (green fluorescence), evident 4 days after exposure to radiation; **b** quantification of Annexin fluorescence intensity in prostate cancer cells exposed to radiation; **c** lack of expression of Annexin in prostate cancer cells, 24 h after exposure to radiation and apalutamide; **d**, **e** western blot images and quantification of cleaved PARP protein expression, 24 h after exposure of 22Rv1 to radiation, Apalutamide, their combination and docetaxel (used as control).

Detection Kit (ab176749) (Abcam, UK) and Cell-IQ MLF live imaging system were used for the detection of cells with Annexin V expression. These experiments showed that prostate cancer cell lines exhibit a delayed onset of the apoptotic process following irradiation. After 4 days, the percentage of cells with apoptotic features was 35 ± 7, 18 ± 5, and 27 ± 7% in the 22Rv1, PC3, and DU145 cells, respectively (Fig. 4a, b).

Since the karyorrhexis and pyknosis identified following irradiation of cancer cells under the presence of apalutamide occur as early as 30 min and persists for 24 h, we investigated whether an early apoptotic response is involved in the phenomenon. Apoptosis was, therefore, assessed at 24 h after irradiation vs. irradiation under the presence of apalutamide. In accordance with the above mentioned results, there was

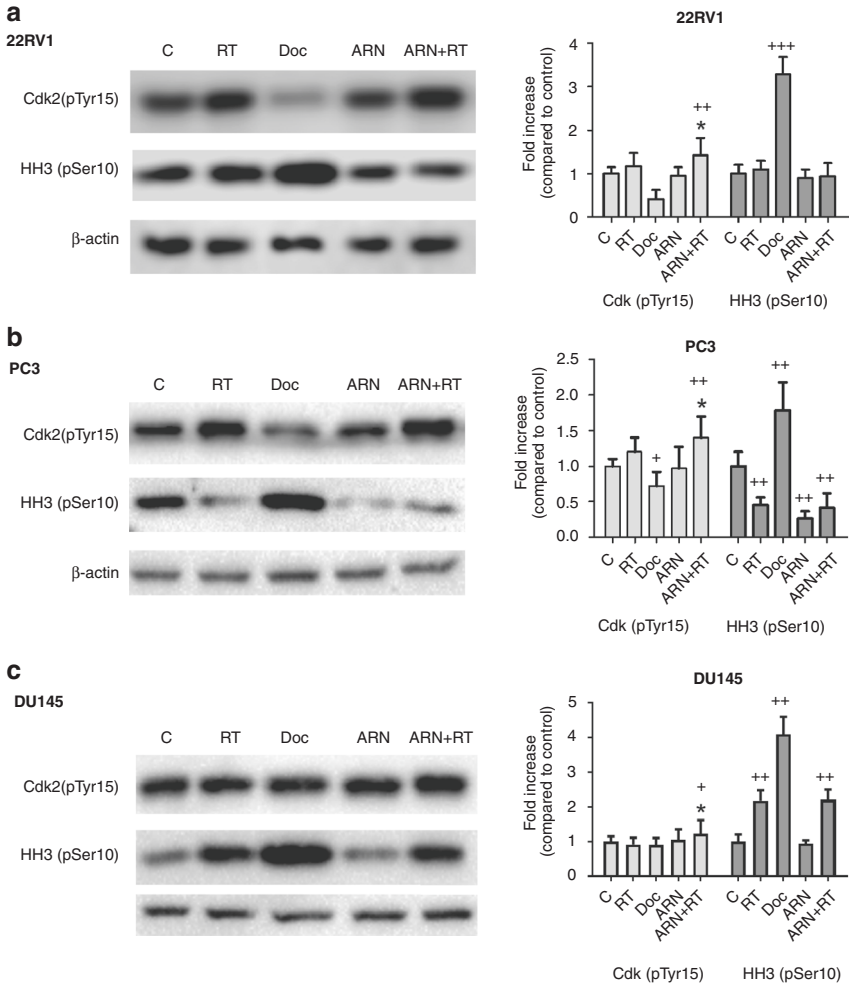

Fig. 5 Treatment with radiation and apalutamide causes G1/S cell cycle arrest. Western blot images and band quantification of phosphorylated Cdk2 and HH3 proteins in 22Rv1 (**a**), PC3 (**b**), and DU145 (**c**) prostate cancer cell lines.

no apoptotic features detectable by the Annexin V method (Fig. 4c).

We further assessed the apoptotic effect at 24 h after irradiation with apalutamide or bicalutamide, by using western blot analysis for cleaved PARP protein, in the 22Rv1 cell line. Again, cleaved PARP was clearly increased after incubation of cells with docetaxel (used as positive control), while radiation whether or not combined with anti-androgens did not show any change (Fig. 4d).

Cell cycle arrest effect

In order to further investigate the pearl-like death effect of combined exposure of prostate cancer cells to radiation and apalutamide, we performed western blot analysis of the expression of Cdk2 (pTyr15) that shows G1/S distribution and of the HH3 (pSer10) that shows G2/M distribution in the cell cycle. Analysis was performed 24 h after irradiation (4 Gy for 22Rv1 and DU147 and 10 Gy for PC3). The effect of docetaxel (5 μM for 24 h) that blocks cells in the G2/M phase was used as a control, and indeed, phosphorylated pCdk2 was decreased and phosphorylated pHH3 was increased in all three cell lines exposed to docetaxel (Fig. 5).

Radiation per se had a minor effect on the cell cycle markers in the 22Rv1 (Fig. 5a) and DU145 cells (Fig. 5c), while a reduction of pHH3 was noted in the PC3 cell line (Fig. 5b). When, however, radiation was combined with apalutamide, a significant increase of the pCdk2 expression was noted, in all three cell lines, compared to the radiation alone (Fig. 5). This shows that combination of the radiation with apalutamide results in G1/S cell cycle arrest, within 24 h after irradiation. This combination had no effect on the G2/M distribution in the cell cycle.

Effect of radiation and anti-androgens on xenografts

Experiments in SCID mice, using 2 Gy irradiation, showed a significant reduction of xenograft growth rate in mice treated with anti-androgens; Fig. 6a. On day 14, xenografts reached a mean fold increase (compared to day 0) of 2.10, 1.72, 1.53, and 1.50 in the 4 groups (control, bicalutamide 50 mg/kg, apalutamide 50 mg/kg, apalutamide 250 mg/kg), respectively. Apalutamide had a significantly stronger radio-sensitising effect compared to bicalutamide ($p < 0.05$). There was no significant difference between the 50 and 250 mg/kg dose schedules of apalutamide. Moreover, these experiments also supported the concept that apalutamide did not further sensitise the already extremely radio-sensitive normal tissues of SCID mice, as mice tolerated equally the 2 Gy dose, whether with or without apalutamide. The shrinkage and necrosis of prostate xenografts is a result of a direct effect of radiation and apalutamide on human cancer cells implanted and not in radio-sensitive SCID mouse fibroblast, as xenografts were growing with minimal evidence of stroma formation.

The experiments in R2G2 mice, using 4 Gy irradiation, showed similarly to the above-mentioned experiments, a significant reduction of xenograft growth rate in mice treated with anti-androgens; Fig. 6b, c. On day 14, xenografts reached a mean

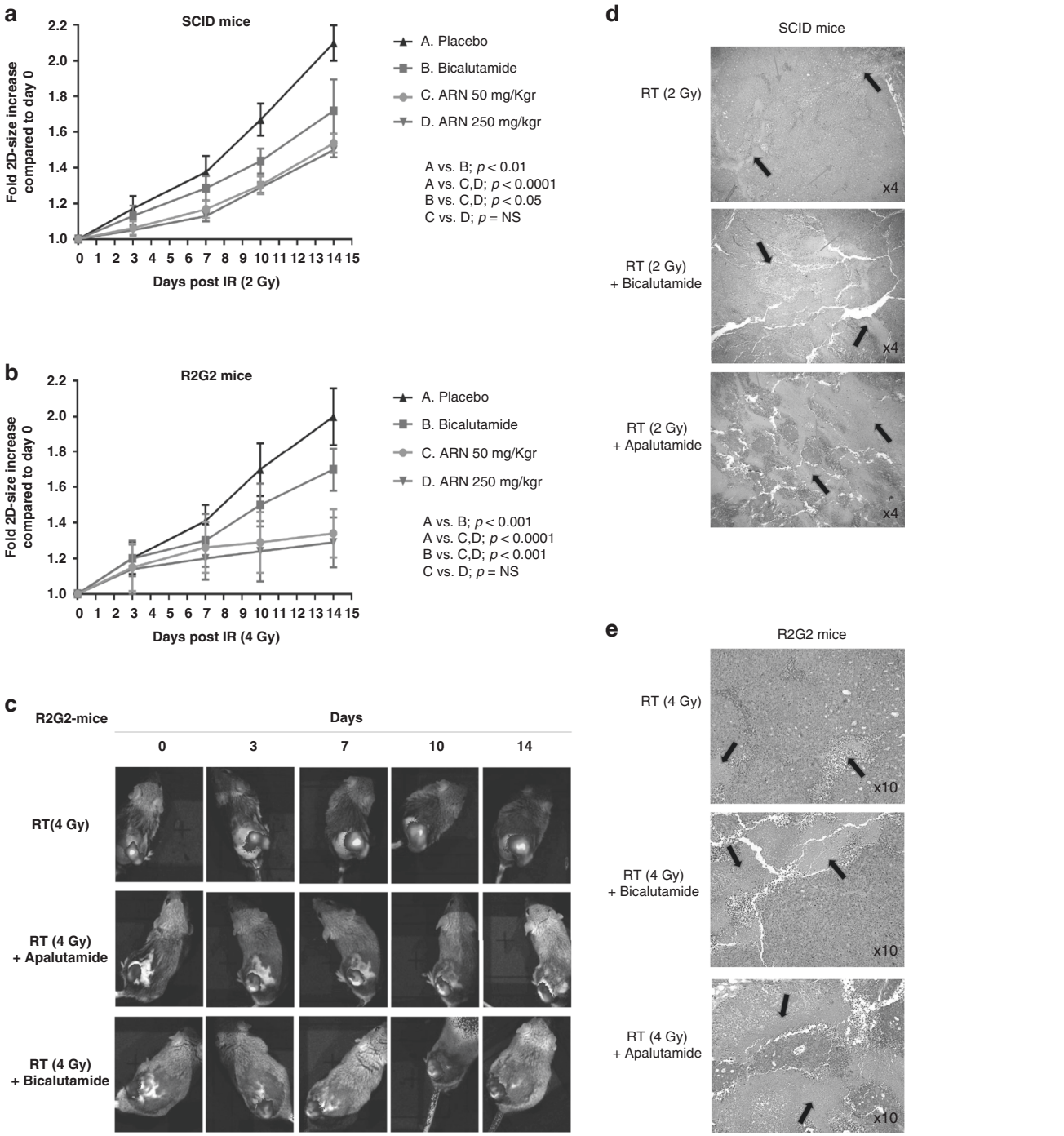

Fig. 6 Apalutamide radio-sensitises PCa cells in vivo. Effect of apalutamide or bicalutamide combination with radiotherapy in 22Rv1 prostate cancer xenografts: **a**, **b** show the growth rate of xenografts growing in SCID and R2G2 mice, respectively, after radiotherapy and its combination with bicalutamide and two-dose schedules of apalutamide; **c** shows typical images of R2G2 mice with fluorescent xenografts followed for 14 days after therapy, with the IVIS kinetics system; **d**, **e** show typical haematoxylin/eosin xenograft tissue sections after radiotherapy and its combination with bicalutamide and apalutamide, where necrosis is indicated with black arrows.

fold increase (compared to day 0) of 2.00, 1.70, 1.34, and 1.29 in the 4 groups, respectively. Apalutamide had a significantly stronger radio-sensitising effect compared to bicalutamide ($p < 0.001$). There was no significant difference between the 50 and 250 mg/kg dose schedules of apalutamide.

Pathology examination of the irradiated xenografts showed that the percentage of xenograft necrosis was significantly increased in irradiated tumours in the presence of bicalutamide ($p < 0.01$), while a dramatic increase of necrosis was evident in mice receiving apalutamide ($p < 0.0001$), regardless of its dose level (Fig. 6d, e). In SCID mice treated with 2 Gy, the mean percentage of necrosis increased from 10% in radiotherapy only tumours to 25, 50, and 55% in the tumour when mice received bicalutamide, apalutamide 50 mg/kg, and apalutamide 250 mg/kg, respectively. In R2G2 mice treated with 4 Gy, the mean percentage of necrosis increased from 15% in radiotherapy only tumours to 30, 60, and 65% in the tumour when mice received bicalutamide, apalutamide 50 mg/kg, and apalutamide 250 mg/kg, respectively.

DISCUSSION

The aim of the current project was to investigate, in vitro and in vivo, the hypothesis that the novel anti-androgen apalutamide is superior to bicalutamide when combined with radiotherapy for the treatment of prostate cancer. Combination of radiotherapy with androgen ablation and bicalutamide is considered the standard of care for patients with high-risk localised (T2, Gleason 8–10) or locally advanced (T3, T4, node-positive) stages of the disease [3–6]. Replacement of bicalutamide with a more potent anti-androgen may provide significant clinical benefits.

Several studies have investigated the mechanisms by which anti-androgens and androgen deprivation enhance the activity of radiotherapy. First Polkinghorn et al. and Goodwin et al. showed that AR signalling activation induces the expression of DNA repair enzymes and anti-androgens can cause significant radio-sensitisation of prostate cancer cells [7, 9]. Since then, several pre-clinical studies using the second-generation anti-androgen enzalutamide confirmed those findings, pointing out the potential use of newly discovered anti-androgens in combination with radiotherapy for better clinical outcomes [17–20, 26]. Moreover, in a recent study Zhang et al. found that exposure to apalutamide of cell lines and prostate cancer tissues results in reduced non-homologous end-joining repair, supporting the use of apalutamide for the localised radiotherapy of prostate cancer patients [27].

Viability and clonogenic assays showed that apalutamide, when combined with radiation at clinically relevant concentrations, significantly suppresses the viability of prostate cancer cells. A strong interaction was noted in the 22Rv1 hormone-dependent cell line. Of interest, a significant potentiation of the combination, although of a lesser magnitude, was noted in the PC3 and DU145 cell line, known to have a hormone-independent behaviour [16]. These findings are in contrast with some studies that found no effect of enzalutamide or apalutamide on the radio-sensitivity of AR-negative cell lines [20, 26, 27]. However, Sekhar et al found that enzalutamide radio-sensitises the DU145 cell line, which is in accordance with our results [19]. Apalutamide induced a higher amount and long persisting DNA double-strand breaks when combined with radiation, as compared to radiation alone. This effect, however, was similar to the one produced by bicalutamide and radiotherapy combination. These findings are in overall agreement with a recently published study by Elsesy et al., where second-generation anti-androgens, like apalutamide and enzalutamide, suppressed the cell growth of irradiated prostate cancer cells (2 Gy) in hormone-sensitive and castration-resistant cell lines [17]. This effect was more prominent compared to bicalutamide. Authors also found that second-generation anti-androgens suppress DNA double-strand break repair better than bicalutamide. Our experiments that applied a much higher dose of radiation (4–10 vs. 2 Gy) did not, however, confirm this latter finding, which may show that, in hypofractionated regimens of radiotherapy, the differential radio-sensitising efficacy between the first- and second-generation anti-androgen is diminished.

The higher efficacy of apalutamide (vs. bicalutamide) combination with radiotherapy against hormone-sensitive and hormone-resistant prostate cancer cells paralleled an early appearance (as early as 30 min from irradiation) of dying cells with karyorrhexis, pyknosis, and pearl-like distribution of fragmented nuclei in the periphery of the cell. Combination of radiation with bicalutamide did not provide any similar effect. This type of cell death has not been reported in other studies. Although in their studies Zhang et al. and Elsesy et al. used apalutamide, they did not report such observations, which may be indicated in the different doses of radiation and apalutamide that were used in the present study [17, 27]. This apalutamide-triggered death pathway was not in the context of an early apoptotic effect and was not related to mitotic catastrophe. Cell cycle experiments did not show a pre-mitotic arrest but rather a G1/S phase cell cycle arrest within 24 h after irradiation. The fact that this death pathway was triggered in all cell lines suggests that a mechanism of apalutamide activity independent of hormone interactions may underlie and may be the key response explaining the superiority of apalutamide as a radio-sensitiser. This death pathway is presumably a different cell death pathway compared to the traditional 'mitotic catastrophe' [28], a process widely recognised as a death pathway induced by radiation that occurs when cells enter mitosis. Whether apalutamide may also have an effect against non-prostate cell lines demands further investigation.

In vivo experiments with immunofluorescent 22Rv1 xenografts implanted on two strains of GEMM were performed. Apalutamide or bicalutamide was delivered with radiotherapy at 2 Gy (the standard dose per fraction used in conventionally fractionated radiotherapy) and at 4 Gy (a dose applied in novel hypofractionated radiotherapy schemes). These two radiation dose levels were applied in xenografts growing in SCID and R2G2 mice, respectively. SCID mice do not tolerate doses >2 Gy delivered to the abdominal area. Both bicalutamide and apalutamide produced a radio-sensitising effect, suppressing the growth rate of xenografts compared to controls. The effect of apalutamide was, however, significantly more robust. The growth suppression was more prominent in R2G2 mice as the radiotherapy dose was 4 Gy compared to the 2 Gy delivered to SCID mice. Of interest, the radio-sensitising effect of apalutamide was more prominent when combined with 4 Gy of radiation, implying a potential robust effect of apalutamide when combined with hypofractionated radiotherapy. Interesting findings were provided after the pathological examination of the irradiated xenografts. The extent of tumour necrosis was threefold higher in tumours treated with apalutamide together with radiation compared to controls and twofold higher than the extent of necrosis noted in tumours treated with bicalutamide.

Our in vitro and in vivo results strongly support the superiority of apalutamide over bicalutamide for combinations of radiotherapy with anti-androgens. Replacement of bicalutamide with a more potent anti-androgen, like apalutamide, shown to better potentiate the activity of radiotherapy, may provide significant clinical benefits for locally advanced disease. Combination of apalutamide with hypofractionated or ultra-hypofractionated radiotherapy [29] may improve prostate cancer curability. Clinical ongoing trials (e.g. NCT03503344) are expected to provide important conclusions regarding the combination of apalutamide with radiotherapy in localised prostate cancer.

DATA AVAILABILITY

All data reported in the study are available in our departments.

REFERENCES

1. Cancer Research UK. Prostate cancer incidence statistics. 2015. https://www.cancerresearchuk.org/health-professional/cancer-statistics/statistics-by-cancer-type/prostate-cancer/incidence. Accessed 8 May 2021.
2. Siegel RL, Miller KD, Jemal A. Cancer statistics, 2020. CA Cancer J Clin. 2020;70:7–30.
3. Warde P, Mason M, Ding K, Kirkbride P, Brundage M, Cowan R, et al. Combined androgen deprivation therapy and radiation therapy for locally advanced prostate cancer: a randomised, phase 3 trial. Lancet. 2011;378:2104–11.
4. Brundage M, Sydes MR, Parulekar WR, Warde P, Cowan R, Bezjak A, et al. Impact of radiotherapy when added to androgen-deprivation therapy for locally advanced prostate cancer: long-term quality-of-life outcomes from the NCIC CTG PR3/MRC PR07 randomized trial. J Clin Oncol. 2015;33:2151–7.
5. Mason MD, Parulekar WR, Sydes MR, Brundage M, Kirkbride P, Gospodarowicz M, et al. Final Report of the Intergroup Randomized Study of Combined Androgen-Deprivation Therapy Plus Radiotherapy Versus Androgen-Deprivation Therapy Alone in Locally Advanced Prostate Cancer. J Clin Oncol. 2015;33:2143–50.
6. Widmark A, Klepp O, Solberg A, Damber J-E, Angelsen A, Fransson P, et al. Endocrine treatment, with or without radiotherapy, in locally advanced prostate cancer (SPCG-7/SFUO-3): an open randomised phase III trial. Lancet. 2009;373:301–8.

7. Polkinghorn WR, Parker JS, Lee MX, Kass EM, Spratt DE, Iaquinta PJ, et al. Androgen receptor signaling regulates DNA repair in prostate cancers. Cancer Discov. 2013;3:1245–53.
8. Spratt DE, Evans MJ, Davis BJ, Doran MG, Lee MX, Shah N, et al. Androgen receptor upregulation mediates radioresistance after ionizing radiation. Cancer Res. 2015;75:4688–96.
9. Goodwin JF, Schiewer MJ, Dean JL, Schrecengost RS, de Leeuw R, Han S, et al. A hormone-DNA repair circuit governs the response to genotoxic insult. Cancer Discov. 2013;3:1254–71.
10. Shore ND, Chowdhury S, Villers A, Klotz L, Siemens DR, Phung D, et al. Efficacy and safety of enzalutamide versus bicalutamide for patients with metastatic prostate cancer (TERRAIN): a randomised, double-blind, phase 2 study. Lancet Oncol. 2016;17:153–63.
11. Smith MR, Saad F, Chowdhury S, Oudard S, Hadaschik BA, Graff JN, et al. Apalutamide treatment and metastasis-free survival in prostate cancer. N Engl J Med. 2018;378:1408–18.
12. Clegg NJ, Wongvipat J, Joseph JD, Tran C, Ouk S, Dilhas A, et al. ARN-509: a novel antiandrogen for prostate cancer treatment. Cancer Res. 2012;72:1494–503.
13. Culig Z, Hoffmann J, Erdel M, Eder IE, Hobisch A, Hittmair A, et al. Switch from antagonist to agonist of the androgen receptor bicalutamide is associated with prostate tumour progression in a new model system. Br J Cancer. 1999;81:242–51.
14. Saad F, Cella D, Basch E, Hadaschik BA, Mainwaring PN, Oudard S, et al. Effect of apalutamide on health-related quality of life in patients with non-metastatic castration-resistant prostate cancer: an analysis of the SPARTAN randomised, placebo-controlled, phase 3 trial. Lancet Oncol. 2018;19:1404–16.
15. Chi KN, Agarwal N, Bjartell A, Chung BH, Pereira de Santana Gomes AJ, Given R, et al. Apalutamide for metastatic, castration-sensitive prostate cancer. N. Engl J Med. 2019;381:13–24.
16. Koukourakis MI, Kakouratos C, Kalamida D, Mitrakas A, Pouliliou S, Xanthopoulou E, et al. Comparison of the effect of the antiandrogen apalutamide (ARN-509) versus bicalutamide on the androgen receptor pathway in prostate cancer cell lines. Anticancer Drugs. 2018;29:323–33.
17. Elsesy ME, Oh-Hohenhorst SJ, Löser A, Oing C, Mutiara S, Köcher S, et al. Second-generation antiandrogen therapy radiosensitizes prostate cancer regardless of castration state through inhibition of DNA double strand break repair. Cancers. 2020;12:2467.
18. Ghashghaei M, Niazi TM, Heravi M, Bekerat H, Trifiro M, Paliouras M, et al. Enhanced radiosensitization of enzalutamide via schedule dependent administration to androgen-sensitive prostate cancer cells. Prostate. 2018;78:64–75.
19. Sekhar KR, Wang J, Freeman ML, Kirschner AN. Radiosensitization by enzalutamide for human prostate cancer is mediated through the DNA damage repair pathway. PLoS ONE. 2019;14:e0214670.
20. Triggiani L, Colosini A, Buglione M, Pasinetti N, Orizio F, Bardoscia L, et al. Exploring the role of enzalutamide in combination with radiation therapy: an in vitro study. Anticancer Res. 2018;38:3487–92.
21. Zachari MA, Chondrou PS, Pouliliou SE, Mitrakas AG, Abatzoglou I, Zois CE, et al. Evaluation of the alamarblue assay for adherent cell irradiation experiments. Dose Response. 2014;12:246–58.
22. Abatzoglou I, Zois CE, Pouliliou S, Koukourakis MI. Establishment and validation of a method for multi-dose irradiation of cells in 96-well microplates. Biochem Biophys Res Commun. 2013;431:456–9.
23. Karagounis IV, Abatzoglou IM, Koukourakis MI. Technical note: Partial body irradiation of mice using a customized PMMA apparatus and a clinical 3D planning/LINAC radiotherapy system. Med Phys. 2016;43:2200.
24. Speers C, Zhao SG, Chandler B, Liu M, Wilder-Romans K, Olsen E, et al. Androgen receptor as a mediator and biomarker of radioresistance in triple-negative breast cancer. npj Breast Cancer. 2017;3:1–10.
25. Nair AB, Jacob S. A simple practice guide for dose conversion between animals and human. J Basic Clin Pharm. 2016;7:27–31.
26. Barrado M, Blanco-Luquin I, Navarrete PA, Visus I, Guerrero-Setas D, Escors D, et al. Radiopotentiation of enzalutamide over human prostate cancer cells as assessed by real-time cell monitoring. Rep Pract Oncol Radiother. 2019;24:221–6.
27. Zhang W, Liao C-Y, Chtatou H, Incrocci L, van Gent DC, van Weerden WM, et al. Apalutamide sensitizes prostate cancer to ionizing radiation via inhibition of non-homologous end-joining DNA repair. Cancers. 2019;11:1593.
28. Castedo M, Perfettini J-L, Roumier T, Andreau K, Medema R, Kroemer G. Cell death by mitotic catastrophe: a molecular definition. Oncogene. 2004;23:2825–37.
29. Morgan SC, Hoffman K, Loblaw DA, Buyyounouski MK, Patton C, Barocas D, et al. Hypofractionated radiation therapy for localized prostate cancer: executive summary of an ASTRO, ASCO, and AUA evidence-based guideline. Pract Radiat Oncol. 2018;8:354–60.

AUTHOR CONTRIBUTIONS

CK: in vitro experiments, animal experiments, analysis and interpretation of data, writing of the paper, approval for submission. DK: confocal imaging experiments, analysis and interpretation of data, writing of the paper, approval for submission. IL: animal experiments, analysis and interpretation of data, writing of the paper, approval for submission. EX: in vitro experiments, western blot analysis, writing of the paper, approval for submission. CN: animal irradiation, writing of the paper, approval for submission. AG: conception and design, analysis and interpretation of data, writing of the paper. MIK: conception and design, analysis and interpretation of data, writing of the paper, study supervision.

FUNDING

The study has been supported by a research grant (ARN-I-15-GRC-001-V02) from Janssen Pharmaceutica NV (Principal Investigator MI Koukourakis).

ETHICS APPROVAL AND CONSENT TO PARTICIPATE

The study has been approved by the local Animal Experimentation Research Committee and the Ethics Committee of the Democritus University of Thrace (AP19/28-7-17). The Veterinary Direction also approved all experimental procedures for Animal Research in the Department of Experimental Surgery at the Democritus University of Thrace.

CONSENT TO PUBLISH

There are no individual person's data included in the paper.

COMPETING INTERESTS

The authors declare no competing interests.

ADDITIONAL INFORMATION

Supplementary information The online version contains supplementary material available at https://doi.org/10.1038/s41416-021-01528-1.

Correspondence and requests for materials should be addressed to M.I.K.

Reprints and permission information is available at http://www.nature.com/reprints

Publisher's note Springer Nature remains neutral with regard to jurisdictional claims in published maps and institutional affiliations.